Prognostic value of a modified-immune scoring system in patients with pathological T4 colorectal cancer

GENDENSUREN DORJKHORLOO[1*], BILGUUN ERKHEM-OCHIR[2*], TAKUYA SHIRAISHI[1*], MAKOTO SOHDA[1], HARUKA OKAMI[1], ARISA YAMAGUCHI[1], IKUMA SHIOI[1], CHIKA KOMINE[1], NOBUHIRO NAKAZAWA[1], NAOYA OZAWA[1], YUTA SHIBASAKI[1], TAKUHISA OKADA[1], KATSUYA OSONE[1], AKIHIKO SANO[1], MAKOTO SAKAI[1], HIROOMI OGAWA[1], TAKEHIKO YOKOBORI[2], KEN SHIRABE[1] and HIROSHI SAEKI[1]

[1]Department of General Surgical Science, Graduate School of Medicine, Gunma University; [2]Division of Integrated Oncology Research, Gunma University Initiative for Advanced Research, Maebashi, Gunma 371-8511, Japan

Received September 26, 2023; Accepted December 13, 2023

DOI: 10.3892/ol.2024.14237

Abstract. Tumor-infiltrating immune cells, such as lymphocytes and macrophages, have been associated with tumor aggressiveness, prognosis and treatment response in colorectal cancer (CRC). An immune scoring system, Immunoscore (IS), based on tumor-infiltrating T cells in stage I-III CRC, was used to predict prognosis. An alternative immune scoring signature of immune activation (SIA) reflects the balance between anti- and pro-tumoral immune components. The present study aimed to evaluate the prognostic value of modified IS (mIS) and modified SIA (mSIA) in locally advanced pathological T4 (pT4) CRC, including stage IV CRC. Immunohistochemical staining for immune cell markers, such as CD3 (pan-T cell marker), CD8 (anti-tumoral cytotoxic T cell marker) and CD163 (tumor-supportive macrophage marker), in specimens from patients with radically resected pT4 CRC at stages II-IV was performed. mIS levels in the T4 CRC cohort were not associated with prognosis. However, low mSIA levels were associated with low survival. Furthermore, low mSIA was an independent predictor of recurrence in patients with radically resected pT4 CRC. In patients with CRC who did not receive postoperative adjuvant chemotherapy, low mSIA was a major poor prognostic factor; however, this was not observed in patients receiving adjuvant chemotherapy. Evaluation of the tumor-infiltrating immune cell population could serve as a valuable marker of recurrence and poor prognosis in patients with locally advanced CRC. mSIA assessment after radical CRC resection may be promising for identifying high-risk patients with pT4 CRC who require aggressive adjuvant chemotherapy.

Correspondence to: Dr Takehiko Yokobori, Division of Integrated Oncology Research, Gunma University Initiative for Advanced Research, 3-39-22 Showa-machi, Maebashi, Gunma 371-8511, Japan
E-mail: bori45@gunma-u.ac.jp

Dr Makoto Sohda, Department of General Surgical Science, Graduate School of Medicine, Gunma University, 3-39-22 Showa-machi, Maebashi, Gunma 371-8511, Japan
E-mail: msohda@gunma-u.ac.jp

[*]Contributed equally

Key words: immune cell infiltration, tumor immunity, prognostic marker, colon cancer, locally advanced colon cancer, Immunoscore, signature of immune activation

Introduction

Tumor-infiltrating immune cells, such as lymphocytes and macrophages, are associated with tumor aggressiveness, prognosis, and treatment response in several cancers, including colorectal cancer (CRC) (1-4). Several factors influence the infiltration of immune cells within the tumor, and shape both pro- and anti-tumoral immune properties (5-10). Aggressive cancer phenotypes, such as epithelial–mesenchymal transition (EMT), have been linked to the degree of immune cell infiltration (11-14). The significant correlation between vascular density and the deposition of tumor-infiltrating lymphocytes has been extensively discussed (15,16). In addition, tumor-infiltrating lymphocytes are associated with good prognosis and sensitivity to anticancer drugs in lung and ovarian cancers (17,18), whereas tumor-infiltrating macrophages are associated with treatment resistance in glioblastoma (19). However, the impact of tumor-infiltrating immune cells on sensitivity to anticancer drugs in CRC, with the frequent use of anticancer therapy for the treatment and prevention of recurrence, has not been thoroughly investigated. Therefore, it is essential to develop an immune scoring system for accurately predicting the treatment response of patients with CRC at a high risk of requiring adjuvant chemotherapy.

Several researchers have used diverse immune cell markers, such as CD3 (pan-T cell marker), CD8 (cytotoxic T cell marker), CD68 (pan-macrophage marker), and CD163 (anti-inflammatory macrophage marker), to analyze the interaction between tumor cells and immune cells in tumor microenvironments (20-24). Immunoscore (IS), an immune scoring system based on the tumor-infiltrating levels of $CD8^+$ and $CD3^+$ T cells in stage I-III CRC, has been established and has indicated a substantial prognostic value for overcoming existing clinical

parameters (25). Moreover, Mezheyeuski *et al* (26) proposed an alternative immune scoring system that reflects the balance between anti- and pro-tumor immune components called the signature of immune activation (SIA). Using multicolor fluorescence staining, the SIA system combines infiltrating anti-tumor $CD8^+$ T cells with tumor-supportive $CD68^+CD163^+$ macrophages in CRC samples. However, whether IS, based on stages I-III CRC samples using dedicated image analysis software, can help predict survival in patients with locally advanced pathological T4 (pT4) CRC, including stage IV CRC, has not been thoroughly investigated. Furthermore, multicolor fluorescence staining was used to assess $CD68^+CD163^+$ tumor-supportive macrophages with respect to SIA, which cannot be assessed by the generally available bright-field observations.

Based on previous reports regarding IS and SIA as promising prognostic immune markers in CRC, we aimed to evaluate the prognostic value of modified IS (mIS) and modified SIA (mSIA) in pT4 stage II-IV CRC using bright-field immunohistochemical immune cell observation, which is commonly used in clinical practice. Therefore, we performed immunohistochemical staining for immune cell markers such as CD3, CD8, and CD163 in surgically resected specimens from patients with pT4 CRC.

Materials and methods

Clinical samples. This study conformed to the Declaration of Helsinki and was approved by the Institutional Review Board for Clinical Research at the Gunma University Hospital (approval number: HS2023-056). Informed consent was obtained for this retrospective study using the opt-out method. This study included 78 patients with primary pT4 CRC who underwent radical surgery at the Gunma University Hospital from July 2013 to February 2020. Patients who received neoadjuvant chemotherapy or radiation therapy and those who did not undergo radical resection for distant metastases were excluded. Clinical data, including patient characteristics (age, sex, body mass index, tumor location, postoperative complications, pathological T stage, tumor size, tumor differentiation, pathological lymph node metastasis, adjuvant chemotherapy, and radical resection margins), were retrieved from medical and surgical records. Histological sections derived from the surgical specimens were employed for immune cell quantification through immunohistochemical staining. For each patient, immune cells were assessed in both the central tumor and the invasive margin from the same section. Follow-up was conducted until May 2023. The time from surgery to death from any cause was defined as overall survival (OS), and cancer-related mortality was defined as cancer-specific survival (CSS). Disease-free survival was defined as the time from surgery to the first documented disease progression, including local recurrence, distant metastasis, or death due to any reason.

Immunohistochemical staining. Paraffin-embedded CRC specimens were cut into 4-μm-thick sections. All sections were incubated at 60˚C for 60 min and deparaffinized using ClearPlus (FALMA, Tokyo, Japan). The sections were rehydrated using a graded series of ethanol and subjected to antigen retrieval using Immunosaver (Nishin EM, Tokyo, Japan) at 98-100˚C for 45 min. To block endogenous peroxidase activity, the sections were incubated with fresh 0.3% hydrogen peroxide in 100% methanol for 30 min at room temperature. After 30 min of blocking with Protein Block Serum-Free Reagent (Agilent, Santa Clara, USA), the specimens were incubated with primary antibodies in REAL Antibody Diluent (Agilent) at 4˚C for 24 h. The following antibodies were used in this study: CD3 antibody (1:1; Ventana, Tucson, USA; 790-4341), CD8 antibody (1:400; Abcam, Cambridge, UK; ab-4055), CD163 antibody (1:500; Cell Signaling Technology, Danvers, USA; CST-93498S), E-cadherin antibody (1:400; Cell Signaling Technology; CST-3195S), and CD31 antibody (1:50; Agilent; M0823). Primary antibody staining was visualized using the Histofine Simple Stain MAX-PO (Multi) Kit (Nichirei, Tokyo, Japan) according to the manufacturer's instructions. The chromogen 3,3-diaminobenzidine tetrahydrochloride (DAB) was applied as a 0.02% solution in 50 mM ammonium acetate-citrate buffer (pH 6.0) containing 0.005% hydrogen peroxide. Finally, the sections were lightly counterstained with Mayer's hematoxylin. Negative controls were incubated without the primary antibody, and no detectable staining was evident.

Image acquisition and semi-quantitative cell counting. For the quantification of tumor-infiltrating $CD3^+$, $CD8^+$, and $CD163^+$ immune cell density, 41 images covering 11.04 mm^2 tissue area were obtained from each CRC slide using an All-in-One Microscope (BZ-X700, KEYENCE; Fig. 1). Four representative region images consisting of 36 views (4 regions x 9 views, total area 9.07 mm^2) of the central tumor area were captured, and five representative region images (total area 1.97 mm^2) of the invasive margin were captured (Fig. 1B). Tumor-infiltrating $CD3^+$, $CD8^+$, and $CD163^+$ immune cell densities in the central tumor and invasive margins were determined using the Hybrid Cell Count Module (KEYENCE) as a semi-automatic image analysis software. The number of tumor-infiltrating immune cells was divided by the total area (mm^2) to calculate the cell density per mm^2.

Analysis procedure of mIS and mSIA based on the tumor-infiltrating immune cell density. The evaluation processes of the mIS and mSIA in this study are shown in Fig. S1. Briefly, tumor-infiltrating $CD3^+$ and $CD8^+$ immune cell densities derived from the central tumor and invasive margins were converted into percentiles, followed by the average calculation of four percentiles: the CD8 CT percentile, CD8 IM percentile, CD3 CT percentile, and CD3 IM percentile (Fig. S1A). The cut-off value of the average mIS was determined to be 25%, according to the original IS report (25). An average mIS percentile of less than 25% was scored as low mIS and a density between 25 and 100% was scored as high mIS (Fig. S1A).

For mSIA evaluation, the formula for the mSIA ratio was as previously described (26); however, tumor-infiltrating $CD163^+$ immune cells were recognized as tumor-supportive macrophages in this study (Fig. S1B). The density of $CD8^+$ immune cells was divided by the sum of the densities of $CD8^+$ and $CD163^+$ immune cells in the central tumor region, which was further converted into percentiles. The cut-off value of the average mIS was determined to be 51.9% according to

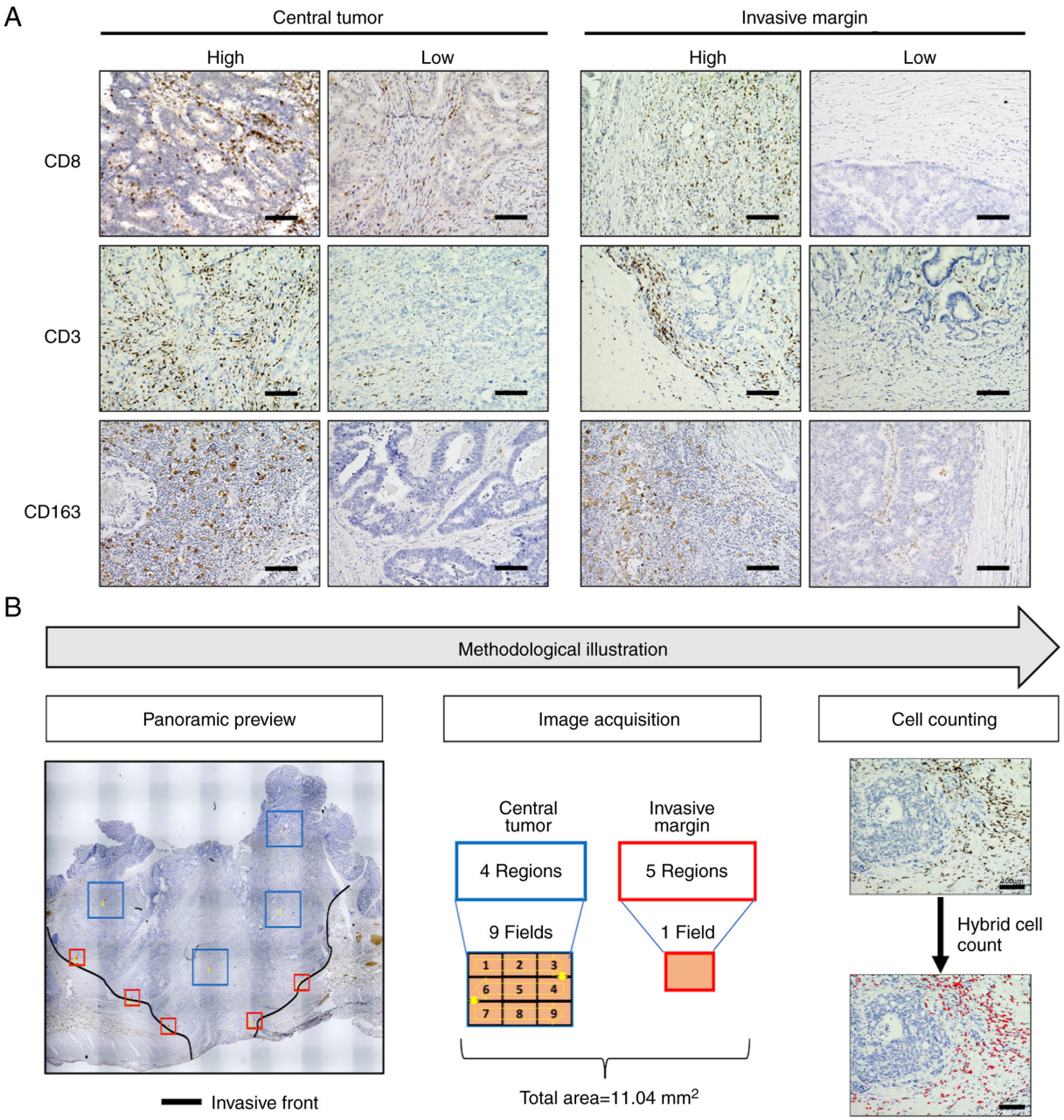

Figure 1. Immune marker staining and illustration of image acquisition and analysis. (A) Representative images of high and low immune cell infiltration of $CD8^+$, $CD3^+$ and $CD163^+$ cells at the central tumor and invasive margin. All images were obtained at a magnification of x200; scale bar, 100 μm. (B) A methodological illustration of image acquisition of $CD8^+$, $CD3^+$ and $CD163^+$ immune cells. The panoramic image was acquired by stitching multiple images captured at x4 magnification, images showing the hybrid cell counting process were obtained at a magnification of x200; scale bar, 100 μm.

the receiver operating characteristic (ROC) curve for cancer recurrence. An average mIS percentile of less than 51.9% was scored as low mSIA, and a density between 51.9 and 100% was scored as high mSIA (Fig. S1B).

Evaluation of E-cadherin expression and CD31-positive microvessel density. To evaluate E-cadherin expression and CD31-positive microvessel density in the CRC tissues, we captured digital images at a magnification of x200 from five representative areas. The number of cells expressing membrane E-cadherin was manually quantified by counting 100 cancer cells in each field, resulting in a total count of 500 cells per slide. The average positive cell count from five fields was used to represent the expression levels of E-cadherin in individual tumors. For microvessel density, we counted the number of CD31-positive vascular structures using five fields using ImageJ software (National Institutes of Health, USA) and calculated the average number of CD31-positive vascular structures. E-cadherin expression and microvessel density were categorized into low and high groups, respectively. The cut-off values of E-cadherin expression and microvessel density were determined according to the ROC curve for cancer recurrence. Among the 78 patients with CRC in this study, 32 (41.0%) were classified into the high E-cadherin expression group and 46 (59.0%) into the low E-cadherin expression group. Regarding the microvessel density, 44 CRC samples (56.4%)

were classified into the high microvessel density group and 34 (43.6%) into the low microvessel density group.

Statistical analysis. Chi-square and Fisher's exact tests were used to determine the association between categorical variables, and the Wilcoxon signed-rank test was used to compare the means of continuous variables between the two groups. Survival rates were analyzed using the Kaplan-Meier method with the log-rank test. Univariate Cox regression analyses were performed to identify the hazard ratio (HR), confidence interval (CI), and P-value for each predictor variable. Factors with P<0.05 in the univariate analyses were included in the multivariate Cox proportional hazards model. The ROC curve was used to determine the cut-off values of mSIA, E-cadherin, and microvessel density that optimally predict cancer recurrence. Statistical analyses were performed using JMP Pro 15 (SAS Institute, Cary, NC, USA). A P-value of <0.05 was considered statistically significant.

Results

Evaluation of mIS and mSIA based on the immunohistochemical staining of tumor-infiltrating CD3$^+$, CD8$^+$, and CD163$^+$ immune cells in pT4 CRC tissues. Fig. 1A shows representative images of immune cell markers, such as CD3, CD8, and CD163, in the central tumor and invasive margin of the surgically resected specimens from patients with pT4 CRC (Fig. 1A). Fig. 1B shows a methodological illustration of the image acquisition and semi-automatic cell counting process from 41 fields of view (Fig. 1B). Based on the counted immune cell density, mIS and mSIA were evaluated according to the analytical procedures (Fig. S1). CD8$^+$ T cell density was significantly higher in the central tumor than in the invasive margin, however no significant difference was observed for the CD3$^+$ cells. In contrast, CD163$^+$ cell densities were significantly higher in the invasive margin than in the central tumor (Fig. S2).

Association of mIS and mSIA with clinicopathological features of patients with pT4 CRC. According to the mIS cut-off value (Fig. S1A), 64 CRC samples (82.1%) were classified into the high mIS group and 14 (17.9%) into the low mIS group (Table I). Information about mIS concerning the clinicopathological characteristics of the patients are summarized in Table I. A low mIS in the total CRC cohort (n=78) was significantly associated with low E-cadherin expression (P=0.0056), microvessel density (P=0.0061), and mSIA (P=0.0066; Table I). The low mIS group with adjuvant chemotherapy was associated with low E-cadherin expression (P=0.0588) and mSIA (P=0.0622), whereas the low mIS group without adjuvant chemotherapy was associated with positive lymph node metastasis (P=0.0390), low E-cadherin expression (P=0.0980), and low microvessel density (P=0.1032; Table I).

According to the cut-off value of mSIA (Fig. S1), 38 CRC samples (48.7%) were classified into the high mSIA group and 40 (51.3%) into the low mSIA group (Table II). Information on mSIA concerning the clinicopathological characteristics of patients is summarized in Table II. Low mSIA was not significantly associated with any existing clinicopathological factors other than mIS (Table II).

Prognostic impact of the mIS and mSIA in patients with pT4 CRC. We evaluated the prognostic value of mIS using survival analysis. Unexpectedly, we did not find a statistically significant difference in overall, cancer-specific, or disease-free survival between patients with high and low mIS scores (Fig. 2, top panel). The significance of mIS as a prognostic factor was analyzed with a focus on the presence or absence of adjuvant chemotherapy. However, similar to the results of the overall case analysis, no significant association was detected between the mIS and survival (Fig. 2, middle and bottom panels).

The same prognostic analyses were performed for the mSIA and mIS. The low mSIA group had significantly poorer overall, cancer-specific, and disease-free survival rates compared to those of the high mSIA group (Fig. 3, top panel). In patients with pT4 CRC who received adjuvant chemotherapy (n=50), low mSIA was not a significant prognostic factor (Fig. 3, middle panel). However, notably, among the patients who did not receive adjuvant chemotherapy (n=20), the low mSIA group had significantly shorter cancer-specific and disease-free survival compared to those of the high mSIA group, and the low mSIA group tended to have poorer OS than the high mSIA group (Fig. 3, bottom panel).

Table III shows the univariate and multivariate analyses of risk factors for different survival rates using the Cox regression model. Univariate analysis revealed that the mSIA was associated with OS (HR=3.6195, 95% CI: 1.2787-10.245; P=0.0154), CSS (HR=3.3266, 95% CI: 1.0118–10.936; P=0.0478), and disease-free survival (HR=2.7883, 95% CI: 1.3938-5.5783; P=0.0037). The multivariate analysis determined that the mSIA was an independent prognostic biomarker for disease-free survival (HR=2.1633, 95% CI, 1.0313-4.5376; P=0.0412; Table III). In contrast, the mIS was not identified as a significant prognostic factor in the same analyses (data not shown).

Discussion

In summary, we evaluated mIS and mSIA using bright-field immunohistochemical staining for CD3, CD8, and CD163 in pathological T4 CRC samples. Contrary to previously reported IS data based on tumor-infiltrating CD3 and CD8 lymphocytes in patients with stage I-III CRC, mIS levels in our T4 CRC cohort were not associated with prognosis. In contrast, in this study, low mSIA levels based on tumor-infiltrating CD8 and CD163 were significantly associated with shorter overall, cancer-specific, and disease-free survival. Moreover, a low mSIA was an independent predictor of recurrence in patients with radically resected pT4 CRC. In patients with CRC who did not receive postoperative adjuvant chemotherapy, a low mSIA was a significantly poor prognostic factor; however, this was not observed in patients receiving adjuvant chemotherapy, suggesting a meaningful relationship between adjuvant chemosensitivity and tumor immune status in CRC.

In this study, we focused on IS (assessing tumor-infiltrating lymphocytes) and SIA (assessing tumor-infiltrating lymphocytes and macrophages), which have previously been reported as promising prognostic markers in stages I-III CRC. In a previous study, a specially developed module was integrated into a commercial image analysis system for the analysis and quantitative evaluation of an IS (25). This study

Table I. Relationship between clinicopathological factors and mIS in patients with pT4 colorectal cancer with and without adjuvant chemotherapy.

	Total patients (n=78)			Adjuvant chemotherapy patients (n=50)			Non-adjuvant chemotherapy patients (n=28)		
Factors	mIS high, n (%) (n=64)	mIS low, n (%) (n=14)	P-value	mIS high, n (%) (n=45)	mIS low, n (%) (n=5)	P-value	mIS high, n (%) (n=19)	mIS low, n (%) (n=9)	P-value
Age, years									
<65	20 (31.2)	5 (35.7)	0.7475[a]	17 (37.8)	3 (60.0)	0.3772[b]	3 (15.8)	2 (22.2)	>0.9999[b]
≥65	44 (68.8)	9 (64.3)		28 (62.2)	2 (40.0)		16 (84.2)	7 (77.8)	
Sex									
Female	29 (45.3)	6 (42.9)	0.8670[a]	22 (48.9)	2 (40.0)	>0.9999[b]	7 (36.8)	3 (33.3)	>0.9999[b]
Male	35 (54.7)	8 (57.1)		23 (51.1)	3 (60.0)		12 (63.2)	6 (66.7)	
Body mass index, kg/m^2									
≥22	24 (37.5)	7 (50.0)	0.3905[a]	17 (37.8)	1 (20.0)	0.6418[b]	7 (36.8)	6 (66.7)	0.2275[b]
<22	40 (62.5)	7 (50.0)		28 (62.2)	4 (80.0)		12 (63.2)	3 (33.3)	
Tumor location									
Colon	46 (71.9)	8 (57.1)	0.2900[a]	33 (73.3)	3 (60.0)	0.6108[b]	13 (68.4)	5 (55.6)	0.6775[b]
Rectum	18 (28.1)	6 (42.9)		12 (26.7)	2 (40.0)		6 (31.6)	4 (44.4)	
Post-operative complications (Clavien-Dindo; grade ≥III)									
Absence	57 (89.1)	12 (85.7)	0.6602[b]	41 (91.1)	4 (80.0)	0.4234[b]	16 (84.2)	8 (88.9)	>0.9999[b]
Presence	7 (10.9)	2 (14.3)		4 (8.9)	1 (20.0)		3 (15.8)	1 (11.1)	
Pathological T stage									
pT4a	31 (48.4)	10 (71.4)	0.1471[b]	25 (55.6)	4 (80.0)	0.3830[b]	6 (31.6)	6 (66.7)	0.1139[b]
pT4b	33 (51.6)	4 (28.6)		20 (44.4)	1 (20.0)		13 (68.4)	3 (33.3)	
Tumor size, mm									
≥50	41 (64.1)	6 (42.9)	0.1461[a]	31 (68.9)	3 (60.0)	0.6498[b]	10 (52.6)	3 (33.3)	0.4348[b]
<50	23 (35.9)	8 (57.1)		14 (31.1)	2 (40.0)		9 (47.4)	6 (66.7)	
Tumor differentiation									
Well or moderately differentiated	31 (48.4)	4 (28.6)	0.2394[b]	22 (48.9)	2 (40.0)	>0.9999[b]	9 (47.4)	2 (22.2)	0.2495[b]
Poorly differentiated	33 (51.6)	10 (71.4)		23 (51.1)	3 (60.0)		10 (52.6)	7 (77.8)	
Pathological lymph node metastasis									
Absence	19 (29.7)	3 (21.4)	0.7456[b]	8 (17.8)	2 (40.0)	0.2581[b]	11 (57.9)	1 (11.1)	0.0390[b,c]
Presence	45 (70.3)	11 (78.6)		37 (82.2)	3 (60.0)		8 (42.1)	8 (88.9)	
Distant metastasis									
Absence	54 (84.4)	10 (71.4)	0.2640[b]	37 (82.2)	4 (80.0)	>0.9999[b]	17 (89.5)	6 (66.7)	0.290[b]
Presence	10 (15.6)	4 (28.6)		8 (17.8)	1 (20.0)		2 (10.5)	3 (33.3)	
Radical resection margin									
Negative	55 (85.9)	10 (71.4)	0.2345[b]	37 (82.2)	4 (80.0)	>0.9999[b]	18 (94.7)	6 (66.7)	0.0841[b]
Positive	9 (14.1)	4 (28.6)		8 (17.8)	1 (20.0)		1 (5.3)	3 (33.3)	
E-cadherin expression									
High	31 (48.4)	1 (7.1)	0.0056[b,c]	22 (48.9)	0 (0.0)	0.0588[b]	9 (47.4)	1 (11.1)	0.0980[b]
Low	33 (51.6)	13 (92.9)		23 (51.1)	5 (100.0)		10 (52.6)	8 (88.9)	
Micro-vessel density									
High	41 (64.1)	3 (21.4)	0.0061[b,c]	29 (64.4)	1 (20.0)	0.1432[b]	12 (63.2)	2 (22.2)	0.1032[b]
Low	23 (35.9)	11 (78.6)		16 (35.6)	4 (80.0)		7 (36.8)	7 (77.8)	

Table I. Continued.

Factors	Total patients (n=78)			Adjuvant chemotherapy patients (n=50)			Non-adjuvant chemotherapy patients (n=28)		
	mIS high, n (%) (n=64)	mIS low, n (%) (n=14)	P-value	mIS high, n (%) (n=45)	mIS low, n (%) (n=5)	P-value	mIS high, n (%) (n=19)	mIS low, n (%) (n=9)	P-value
mSIA									
High	36 (56.3)	2 (14.3)	0.0066[b,c]	30 (66.7)	1 (20.0)	0.0622[b]	6 (31.6)	1 (11.1)	0.3715[b]
Low	28 (43.7)	12 (85.7)		15 (33.3)	4 (80.0)		13 (68.4)	8 (88.9)	

[a]χ^2 test; [b]Fisher's exact test. [c]P<0.05. mIS, modified Immunoscore; mSIA, modified signature of immune activation.

validated the prognostic value of the mIS assessed only using commercial-based image analysis software without a specially developed module and a few technical differences regarding the staining procedure (antigen retrieval and incubation time). We believe that our mIS resembles the IS evaluation system; however, contrary to our expectations, mIS was not a significant prognostic biomarker in our radically resected pT4 CRC cohort. This might be because our cohort only consisted of patients with stage II-IV CRC with pT4, which differs from those in previous research, which included patients with stage I-III CRC.

In contrast, a previous study on SIA utilized fluorescence multiplex staining to identify and determine $CD68^+$ $CD163^+$ anti-inflammatory M2-like macrophages quantitatively and performed a predictive analysis of SIA in patients with stage I-III CRC (26). This study assessed tumor-infiltrating $CD163^+$ cells as anti-inflammatory macrophages using bright-field immunohistochemical observation. Compared to the original SIA, our mSIA has some differences, such as the single-color DAB staining detection of immune cells in a sequential section. We also did not stain the CD68 marker, as it is considered a global macrophage marker (27,28). We believe that single staining of $CD163^+$ cells can potentially represent M2-like phenotypic populations. Many investigators have already used CD163 as a marker of M2-like macrophages, showing its prognostic significance in several cancers (29-32). Thus, we believe that our mSIA, based on $CD8^+$ and $CD163^+$ immune cells, could have the same efficiency as the original SIA. Consistent with our understanding, we found that the mSIA remarkably predicted poor prognosis and recurrence in patients with pT4 CRC. Although we expect that mIS and mSIA may be promising biomarkers that sensitively reflect the local tumor immune status of advanced CRC, including stage IV CRC, this was a retrospective observational study with a limited number of patients. Future studies are needed to prospectively investigate the prognostic and predictive potential of the mSIA and mIS in a larger number of advanced CRC specimens.

Our findings showed that the mSIA, a composite assessment of cytotoxic T cells and macrophages, was not significantly associated with existing clinical factors. In contrast, cases with low mIS, based on low T cell infiltration levels, showed low E-cadherin expression. T cells are recognized as target cells activated by immune checkpoint inhibitors, and the inactivation (exhaustion) of T cells is reportedly triggered by transforming growth factor-beta (TGF-β) signaling (33,34). Moreover, TGF-β signaling activation in tumor microenvironments can cause epithelial-mesenchymal transition (EMT), characterized by the loss of epithelial marker expression, increased migration and invasive ability, therapeutic resistance on the cancer cell side, and suppression of anti-tumor T cell immunity on the immune cell side (35-37). These findings suggest that EMT induction by activating TGF-β signaling in the tumor microenvironment might be one of the reasons underlying low E-cadherin expression in patients with low mIS.

Endothelial cells are crucial in controlling oxygen delivery to and circulating cell infiltration in the tissues (9,10). Furthermore, endothelial cells actively participate in immune responses by regulating immune cell trafficking and activation (8,10,38,39). Microvessel density, evaluated using CD31 staining, was lower in patients with low mIS than in those with high mIS. Our findings coincide with those of previous reports demonstrating that a high microvessel density is correlated with an increased number of tumor-infiltrating lymphocytes in various types of solid cancers (15,16). These reports propose an explanation for the association between mIS levels and the abundance of tumor-infiltrating lymphocytes.

Previous reports on melanoma have described that cases with low SIA, based on single-cell RNA sequencing data, are more resistant to immune checkpoint inhibitors (26). The current mechanism of action of immune checkpoint inhibitors includes the activation of cytotoxic T lymphocytes by antibody drugs targeting immune checkpoint proteins. Many investigators have reported low levels of tumor-infiltrating cytotoxic T cells being associated with low sensitivity to immune checkpoint inhibitors such as anti-PD-1 and anti-PD-L1 antibodies (40-43). However, the impact of tumor-infiltrating immune cells on the sensitivity to cytotoxic anticancer drugs has not been thoroughly investigated in patients with CRC. In the present study, we analyzed whether mIS and mSIA are associated with sensitivity to cytotoxic anticancer drugs in patients with radically resected pT4 CRC, with and without postoperative adjuvant chemotherapy. Our findings in the total pT4 CRC cohort, including stage IV cases (n=78), showed that patients with CRC and high mSIA had a better prognosis than those with low mSIA, consistent with the results of a previous report in a stage I-III CRC cohort. Thus, high mSIA predicted better survival because high mSIA might reflect a tumor

Table II. Relationship between clinicopathological factors and mSIA in patients with pT4 colorectal cancer with and without adjuvant chemotherapy.

	Total patients (n=78)			Adjuvant chemotherapy patients (n=50)			Non-adjuvant chemotherapy patients (n=28)		
Factors	mSIA high, n (%) (n=38)	mSIA low, n (%) (n=40)	P-value	mSIA high, n (%) (n=31)	mSIA low, n (%) (n=19)	P-value	mSIA high, n (%) (n=7)	mSIA low, n (%) (n=21)	P-value
Age, years									
<65	13 (34.2)	12 (30.0)	0.6904[a]	12 (38.7)	8 (42.1)	0.8121[a]	1 (14.3)	4 (19.0)	>0.9999[b]
≥65	25 (65.8)	28 (70.0)		19 (61.3)	11 (57.9)		6 (85.7)	17 (81.0)	
Sex									
Female	15 (39.5)	20 (50.0)	0.3496[a]	13 (41.9)	12 (63.2)	0.1434[a]	2 (28.6)	8 (38.1)	>0.9999[b]
Male	23 (60.5)	20 (50.0)		18 (58.1)	7 (36.8)		5 (71.4)	13 (61.9)	
Body mass index, kg/m^2									
≥22	16 (42.1)	15 (37.5)	0.6778[a]	13 (41.9)	5 (26.3)	0.2586[a]	3 (42.9)	10 (47.6)	>0.9999[b]
<22	22 (57.9)	25 (62.5)		18 (58.1)	14 (73.7)		4 (57.1)	11 (52.4)	
Tumor location									
Colon	28 (73.7)	26 (65.0)	0.4053[a]	24 (77.4)	12 (63.2)	0.2796[a]	4 (57.1)	14 (66.7)	0.6744[b]
Rectum	10 (26.3)	14 (35.0)		7 (22.6)	7 (36.8)		3 (42.9)	7 (33.3)	
Post-operative complications (Clavien-Dindo; grade ≥III)									
Absence	34 (89.5)	35 (87.5)	>0.9999[b]	29 (93.6)	16 (84.2)	0.3551[b]	5 (71.4)	19 (90.5)	0.2530[b]
Presence	4 (10.5)	5 (12.5)		2 (6.4)	3 (15.8)		2 (28.6)	2 (9.5)	
Pathological T stage									
pT4a	19 (50.0)	22 (55.0)	0.6584[a]	17 (54.8)	12 (63.2)	0.5618[a]	2 (28.6)	10 (47.6)	0.6618[b]
pT4b	19 (50.0)	18 (45.0)		14 (45.2)	7 (36.8)		5 (71.4)	11 (52.4)	
Tumor size, mm									
≥50	25 (65.8)	22 (55.0)	0.3296[a]	21 (67.7)	13 (68.4)	0.9601[a]	4 (57.1)	9 (42.9)	0.6703[b]
<50	13 (34.2)	18 (45.0)		10 (32.3)	6 (31.6)		3 (42.9)	12 (57.1)	
Tumor differentiation									
Well or moderately differentiated	17 (44.7)	18 (45.0)	0.9814[a]	14 (45.2)	10 (52.6)	0.6078[a]	3 (42.9)	8 (38.1)	>0.9999[b]
Poorly differentiated	21 (55.3)	22 (55.0)		17 (54.8)	9 (47.4)		4 (57.1)	13 (61.9)	
Pathological lymph node metastasis									
Absence	10 (26.3)	12 (30.0)	0.7176[a]	6 (19.3)	4 (21.0)	>0.9999[b]	4 (57.1)	8 (38.1)	0.4184[b]
Presence	28 (73.7)	28 (70.0)		25 (80.7)	15 (79.0)		3 (42.9)	13 (61.9)	
Distant metastasis									
Absence	33 (86.8)	31 (77.5)	0.2794[a]	26 (83.9)	15 (79.0)	0.7152[b]	7 (100.0)	16 (76.2)	0.2895[b]
Presence	5 (13.2)	9 (22.5)		5 (16.1)	4 (21.0)		0 (0.0)	5 (23.8)	
Radical resection margin									
Negative	34 (89.5)	31 (77.5)	0.2259[b]	27 (87.1)	14 (73.7)	0.2729[b]	7 (100.0)	17 (81.0)	0.5453[b]
Positive	4 (10.5)	9 (22.5)		4 (12.9)	5 (26.3)		0 (0.0)	4 (19.0)	
E-cadherin expression									
High	18 (47.4)	14 (35.0)	0.2665[a]	14 (45.2)	8 (42.1)	0.8325[a]	4 (57.1)	6 (28.6)	0.2075[b]
Low	20 (52.6)	26 (65.0)		17 (54.8)	11 (57.9)		3 (42.9)	15 (71.4)	
Micro-vessel density									
High	22 (57.9)	22 (55.0)	0.7966[a]	18 (58.1)	12 (63.2)	0.7207[a]	4 (57.1)	10 (47.6)	>0.9999[b]
Low	16 (42.1)	18 (45.0)		13 (41.9)	7 (36.8)		3 (42.9)	11 (52.4)	

Table II. Continued.

Factors	Total patients (n=78)			Adjuvant chemotherapy patients (n=50)			Non-adjuvant chemotherapy patients (n=28)		
	mSIA high, n (%) (n=38)	mSIA low, n (%) (n=40)	P-value	mSIA high, n (%) (n=31)	mSIA low, n (%) (n=19)	P-value	mSIA high, n (%) (n=7)	mSIA low, n (%) (n=21)	P-value
mIS									
High	36 (94.7)	28 (70.0)	0.0066[b,c]	30 (96.8)	15 (79.0)	0.0622[b]	6 (85.7)	13 (61.9)	0.3715[b]
Low	2 (5.3)	12 (30.0)		1 (3.2)	4 (21.0)		1 (14.3)	8 (38.1)	

[a]χ^2 test; [b]Fisher's exact test. [c]P<0.05. mIS, modified Immunoscore; mSIA, modified signature of immune activation.

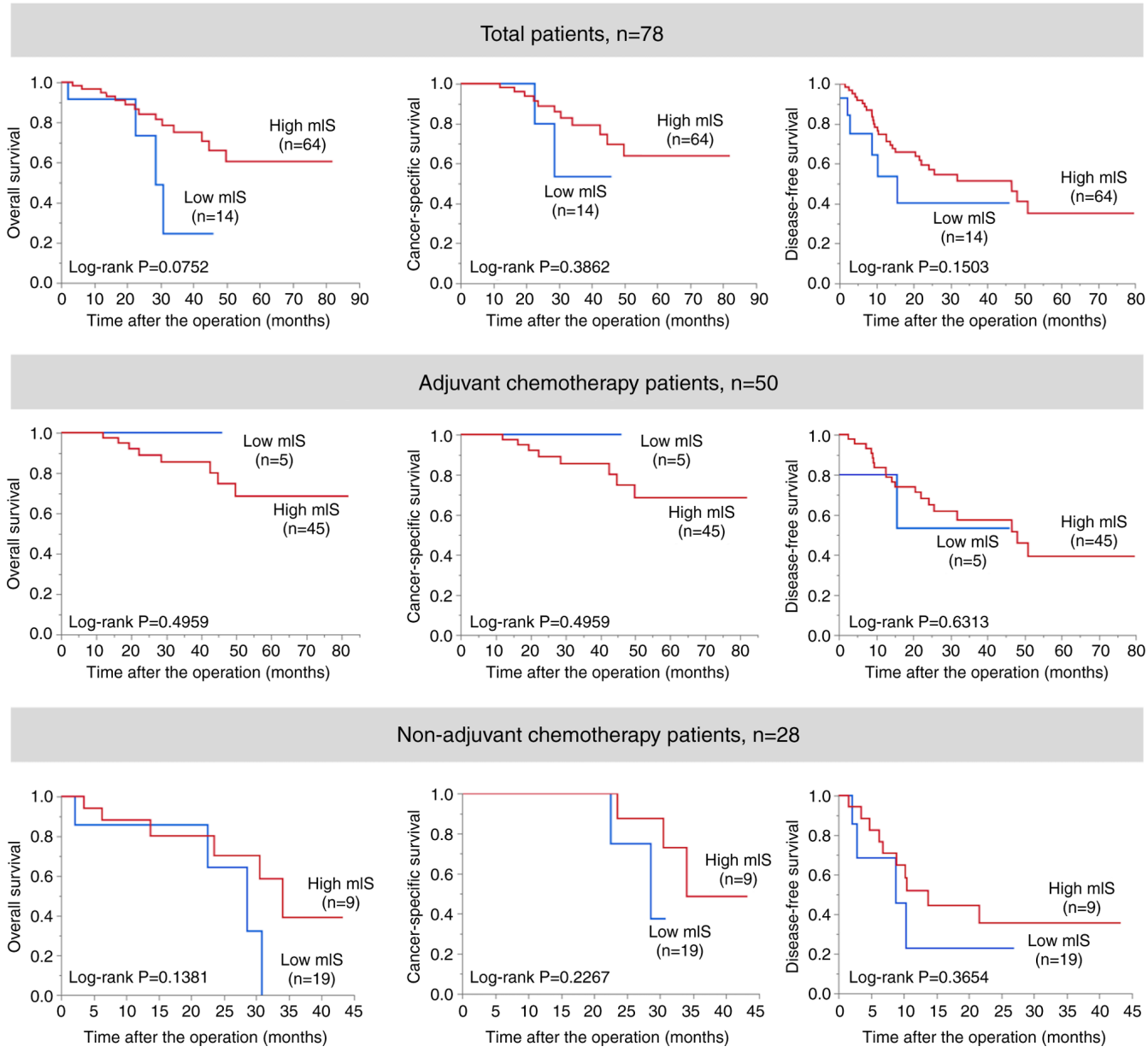

Figure 2. Kaplan-Meier survival curves stratified according to high and low mIS. The top panel shows the overall (left), cancer-specific (middle) and disease-free (right) survival of all patients with pT4 CRC (n=78), according to mIS. The middle panel shows the overall (left), cancer-specific (middle) and disease-free (right) survival of patients with pT4 CRC with postoperative adjuvant chemotherapy (n=50), according to mIS. Patients who underwent adjuvant treatment exhibited indistinguishable overall and cancer-specific survival rates. Within this specific subgroup, all deceased patients succumbed to causes directly linked to cancer. The bottom panel shows the overall (left), cancer-specific (middle) and disease-free (right) survival of patients with pT4 CRC without postoperative adjuvant chemotherapy (n=28), according to mIS. mIS, modified Immunoscore; CRC, colorectal cancer.

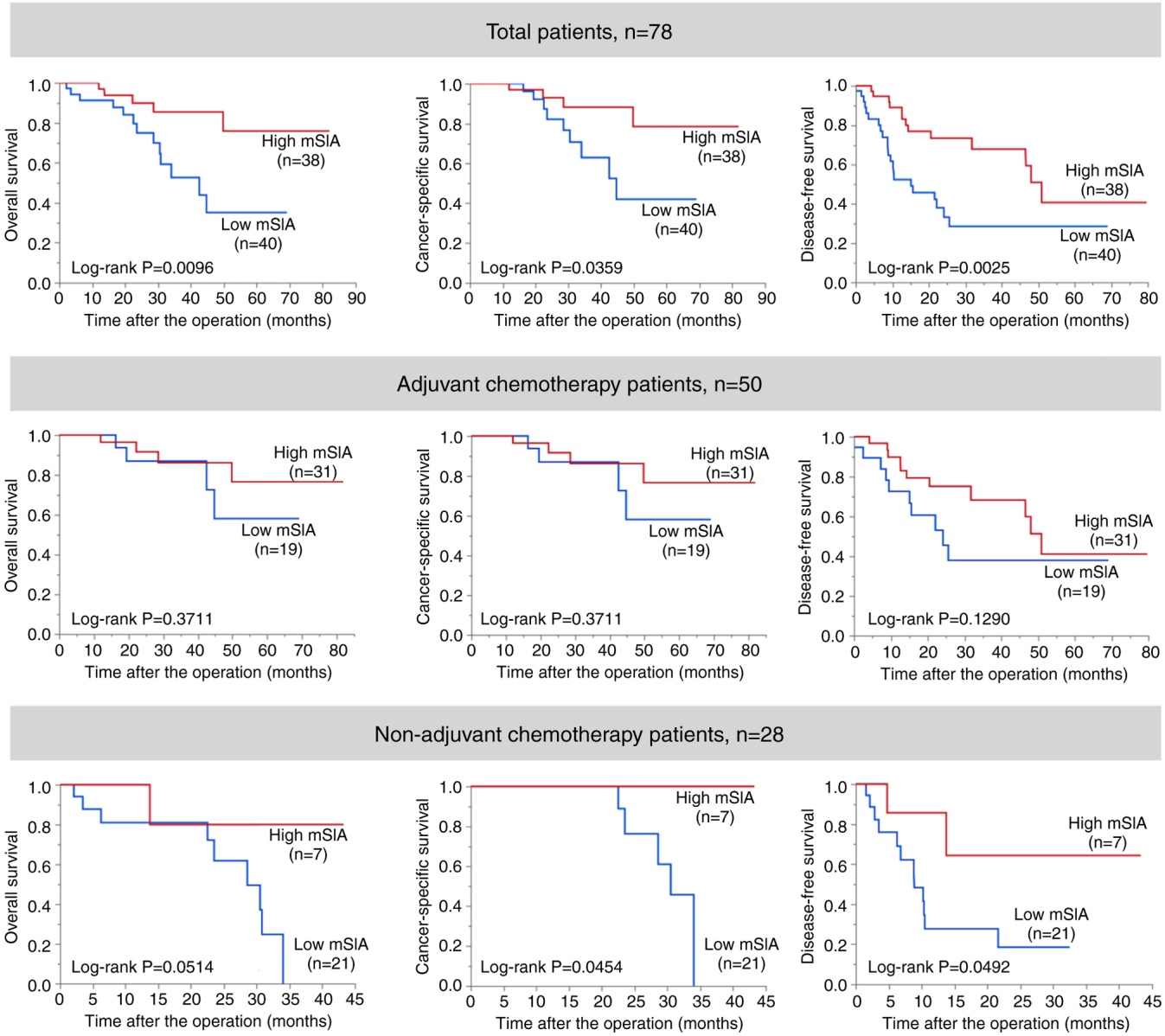

Figure 3. Kaplan-Meier survival curves stratified according to high and low mSIA. The top panel shows the overall (left), cancer-specific (middle) and disease-free (right) survival of all patients with pT4 CRC (n=78), according to mSIA. The middle panel shows the overall (left), cancer-specific (middle) and disease-free (right) survival of patients with pT4 CRC with postoperative adjuvant chemotherapy (n=50), according to mSIA. Patients who underwent adjuvant treatment exhibited indistinguishable overall and cancer-specific survival rates. Within this specific subgroup, all deceased patients succumbed to causes directly linked to cancer. The bottom panel shows the overall (left), cancer-specific (middle) and disease-free (right) survival of patients with pT4 CRC without postoperative adjuvant chemotherapy (n=28), according to mSIA. mSIA, modified signature of immune activation; CRC, colorectal cancer.

microenvironment with high anti-tumor ($CD8^+$ cells) components and low pro-tumoral ($CD163^+$ cells) components. The mSIA was not associated with prognosis in patients receiving adjuvant chemotherapy (n=50). Notably, among patients with pT4 CRC who received non-adjuvant chemotherapy (n=28), the low mSIA group had significantly shorter survival than the high mSIA group. Among patients with low mSIA (n=40), the median disease-free survival time in patients undergoing adjuvant chemotherapy (n=19, 24.17 months) was higher than that in patients who did not receive adjuvant chemotherapy (n=21, 8.87 months; Fig. 3), suggesting that the tumor-infiltrating immune cells might be sensitive to adjuvant chemotherapy with cytotoxic anticancer drugs. Therefore, based on our findings, we suggest that active consideration of postoperative adjuvant chemotherapy for low mSIA cases with a high recurrence risk may improve the prognosis of advanced CRC.

This study has some limitations. First, this was a retrospective, single-institution study, and only patients with radically resected pT4 CRC were recruited. These subjects may have underestimated the significance of the mSIA and mIS in CRC. However, focusing only on stage II-IV pT4 CRCs was a unique feature of this study because the importance of tumor-infiltrating immune cells in stages I-III has already been investigated and reported in many cases. Second, in the present study we did not evaluate the microsatellite instability (MSI) and mismatch repair (MMR) status. Several studies demonstrated that MSI and MMR status are known to be associated with the presence of tumor infiltrated immune cells, treatment

Table III. Univariate and multivariate analyses of clinicopathological factors affecting survival following surgery in patients with pT4 colorectal cancer.

	Overall survival						Cancer-specific survival						Disease-free survival					
	Univariate analysis			Multivariate analysis			Univariate analysis			Multivariate analysis			Univariate analysis			Multivariate analysis		
Factors	HR	95% CI	P-value	HR	95% CI	P-value	HR	95% CI	P-value	HR	95% CI	P-value	HR	95% CI	P-value	HR	95% CI	P-value
Age, years																		
<65	1		0.7592				1		0.9705				1		0.2888			
≥65	1.1665	0.4355-3.1247					0.9790	0.3180-3.0140					1.5077	0.7060-3.2198				
Sex																		
Female	1		0.4168				1		0.8075				1		0.6988			
Male	1.4818	0.5734-3.8294					1.1453	0.3843-3.4135					1.1427	0.5813-2.2463				
Body mass index, kg/m^2																		
≥22	1		0.2725				1		0.2311				1		0.4456			
<22	1.7346	0.6486-4.6391					2.0578	0.6315-6.7053					1.3041	0.6592-2.5798				
Tumor location																		
Colon	1		0.0822				1		0.0822				1		0.2294			
Rectum	2.6407	0.8835-7.8926					2.6407	0.8835-7.8926					1.5263	0.7659-3.0416				
Post-operative complications (Clavien-Dindo; grade ≥III)																		
Absence	1		0.7315				1		0.4824				1		0.8340			
Presence	0.7720	0.1760-3.3851					0.4801	0.0619-3.7196					1.1179	0.3941-3.1711				
Pathological T stage																		
pT4a	1		0.9876				1		0.9021				1		0.4940			
pT4b	0.9923	0.3768-2.6131					1.0747	0.3406-3.3909					0.7851	0.3925-1.5703				
Tumor size, mm																		
≥50	1		0.0147[a]	1		0.0817	1		0.0710				1		0.0041[a]	1		0.0312[a]
<50	3.3915	1.2711-9.0505		2.4931	0.8913-6.9731		2.8030	0.9156-8.5811					2.7130	1.3721-5.3641		2.1633	1.0723-4.3644	
Tumor differentiation																		
Well or moderately differentiated	1		0.2261				1		0.1927				1		0.0470			
Poorly differentiated	1.8429	0.6847-4.9599					2.2050	0.6710-7.2461					2.1064	1.0099-4.3936				

Table III. Continued.

	Overall survival						Cancer-specific survival						Disease-free survival					
	Univariate analysis			Multivariate analysis			Univariate analysis			Multivariate analysis			Univariate analysis			Multivariate analysis		
Factors	HR	95% CI	P-value	HR	95% CI	P-value	HR	95% CI	P-value	HR	95% CI	P-value	HR	95% CI	P-value	HR	95% CI	P-value
Pathological lymph node metastasis																		
Absence	1		0.6506				1		0.7365				1		0.0648			
Presence	1.3356	0.3817-4.6731					1.2989	0.2830-5.9610					2.4500	0.9465-6.3420				
Distant metastasis																		
Absence	1		0.0218[a]	1		0.1006	1		0.0497[a]	1		0.1055	1		0.0011[a]	1		0.0040[a]
Presence	3.0515	1.1766-7.9141		2.3333	0.8486-6.4157		3.0867	1.0014-9.5148		2.5927	0.8180-8.2178		3.4543	1.6390-7.2799		3.0750	1.4314-6.6058	
Adjuvant chemotherapy																		
Presence	1		0.0015[a]	1		0.0229[a]	1		0.0909				1		0.0078[a]	1		0.0645
Absence	5.4394	1.9150-15.450		3.7504	1.2009-11.712		2.8722	0.8453-9.7587					2.6138	1.2881-5.3036		2.0519	0.9576-4.3968	
Radical resection margin																		
Negative	1		0.4011				1		0.7294				1		0.4849			
Positive	1.5295	0.5671-4.1253					1.2337	0.3753-4.0548					1.3290	0.5982-2.9528				
E-cadherin expression																		
High	1		0.1490				1		0.2608				1		0.1010			
Low	2.2695	0.7455-6.9087					2.0993	0.5763-7.6466					1.8479	0.8871-3.8495				
Micro-vessel density																		
High	1		0.3024				1		0.5731				1		0.5825			
Low	1.6379	0.6412-4.1839					1.3822	0.4483-4.2613					1.2157	0.6058-2.4394				
mIS																		
High	1		0.0877				1		0.3958				1		0.1573			
Low	2.6898	0.8640-8.3740					1.9427	0.4194-8.9969					1.9045	0.7798-4.6511				
mSIA																		
High	1		0.0154[a]	1		0.2966	1		0.0478[a]	1		0.0807	1		0.0037[a]	1		0.0412[a]
Low	3.6195	1.2787-10.245		1.8865	0.5727-6.2138		3.3266	1.0118-10.936		2.9588	0.8760-9.9937		2.7883	1.3938-5.5783		2.1633	1.0313-4.5376	

[a]P<0.05. mIS, modified Immunoscore; mSIA, modified signature of immune activation; HR, hazard ratio.

response, and overall prognosis in CRC (44,45). Third, this study focused on the prognostic significance of immune cells in advanced CRC; however, we only analyzed cases whose surgical specimens were available following radical resection, which might have caused a sampling bias. In the future, it is necessary to further investigate whether mSIA and mIS are associated with drug sensitivity and prognosis in stage I-IV CRC using both pretreatment biopsy and resected tumor samples. Finally, the mSIA and mIS evaluations conducted in this study differed from those in previous reports.

In conclusion, we showed a remarkably good prognostic value of high mSIA based on high $CD8^+$ T cell and low $CD163^+$ macrophage infiltration in patients with radically resected pT4 CRC. Evaluation of tumor-infiltrating immune cells may be a useful predictive marker of recurrence and poor prognosis in patients with locally advanced CRC. Moreover, a low mSIA was associated with poor survival and recurrence in patients with pT4 CRC who did not receive adjuvant therapy, unlike in those who received chemotherapy. Pretreatment mSIA assessment following radical CRC resection shows potential in identifying high-risk patients with pT4 CRC who require adjuvant chemotherapy.

Acknowledgements

The authors would like to thank Ms. Mariko Nakamura and Ms. Kao Abe (Department of General Surgical Science, Graduate School of Medicine, Gunma University, Maebashi, Japan), and Ms. Yukiko Suto (Laboratory for Analytical Instruments, Gunma University, Maebashi, Japan) for their assistance in immunohistochemical staining. The authors would also like to thank Ms. Kyoko Miyoshi, Ms. Miyoko Suzuki, Ms. Chiho Noguchi and Ms. Saori Suto (Division of Integrated Oncology Research, Gunma University Initiative for Advanced Research, Maebashi, Japan), and Ms. Sayaka Okada and Ms. Harumi Kanai (Department of General Surgical Science, Graduate School of Medicine, Gunma University, Maebashi, Japan) for their administrative support.

Funding

The present study was supported by the Grants-in-Aid for Scientific Research from the Japan Society for the Promotion of Science (JSPS; grant nos. 23K14610, 22H02912, 22K08766 and 21K08749).

Availability of data and materials

The datasets used and/or analyzed during the current study are available from the corresponding author on reasonable request.

Authors' contributions

GD and HO collected and analyzed the image data. GD, BEO, TS and TY analyzed and interpreted the data. TS, MSo and TY confirm the authenticity of all the raw data. GD, BEO, TS and TY drafted the manuscript. MSo, TS, BEO, TY, KS and HS conceptualized the study. TS, AY, IS, CK, NN, NO, YS, TO, KO, AS, MSa, HO and MSo contributed to sample collection and data analysis. All authors read and approved the final manuscript.

Ethics approval and consent to participate

The present study conformed to the Declaration of Helsinki and was approved by the Institutional Review Board for Clinical Research at the Gunma University Hospital (approval no. HS2023-056; Maebashi, Japan). Informed consent was obtained for this retrospective study using the opt-out method.

Patient consent for publication

Not applicable.

Competing interests

The authors declare that they have no competing interests.

References

1. Laghi L, Negri F, Gaiani F, Cavalleri T, Grizzi F, De' Angelis GL and Malesci A: Prognostic and predictive cross-roads of microsatellite instability and immune response to colon cancer. Int J Mol Sci 21: 9680, 2020.
2. Brummel K, Eerkens AL, de Bruyn M and Nijman HW: Tumour-infiltrating lymphocytes: From prognosis to treatment selection. Br J Cancer 128: 451-458, 2023.
3. Zhang Q and Sioud M: Tumor-associated macrophage subsets: Shaping polarization and targeting. Int J Mol Sci 24: 7493, 2023.
4. Daitoku N, Miyamoto Y, Hiyoshi Y, Tokunaga R, Sakamoto Y, Sawayama H, Ishimoto T, Baba Y, Yoshida N and Baba H: Preoperative skeletal muscle status is associated with tumor-infiltrating lymphocytes and prognosis in patients with colorectal cancer. Ann Gastroenterol Surg 6: 658-666, 2022.
5. Melssen MM, Sheybani ND, Leick KM and Slingluff CL Jr: Barriers to immune cell infiltration in tumors. J Immunother Cancer 11: e006401, 2023.
6. Xiao Z, Todd L, Huang L, Noguera-Ortega E, Lu Z, Huang L, Kopp M, Li Y, Pattada N, Zhong W, *et al*: Desmoplastic stroma restricts T cell extravasation and mediates immune exclusion and immunosuppression in solid tumors. Nat Commun 14: 5110, 2023.
7. Mao X, Xu J, Wang W, Liang C, Hua J, Liu J, Zhang B, Meng Q, Yu X and Shi S: Crosstalk between cancer-associated fibroblasts and immune cells in the tumor microenvironment: New findings and future perspectives. Mol Cancer 20: 131, 2021.
8. Bais C, Mueller B, Brady MF, Mannel RS, Burger RA, Wei W, Marien KM, Kockx MM, Husain A, Birrer MJ, *et al*: Tumor microvessel density as a potential predictive marker for bevacizumab benefit: GOG-0218 biomarker analyses. J Natl Cancer Inst 109: djx066, 2017.
9. Zeng Q, Mousa M, Nadukkandy AS, Franssens L, Alnaqbi H, Alshamsi FY, Safar HA and Carmeliet P: Understanding tumour endothelial cell heterogeneity and function from single-cell omics. Nat Rev Cancer 23: 544-564, 2023.
10. Hendry SA, Farnsworth RH, Solomon B, Achen MG, Stacker SA and Fox SB: The role of the tumor vasculature in the host immune response: Implications for therapeutic strategies targeting the tumor microenvironment. Front Immunol 7: 621, 2016.
11. Heryanto YD and Imoto S: The transcriptome signature analysis of the epithelial-mesenchymal transition and immune cell infiltration in colon adenocarcinoma. Sci Rep 13: 18383, 2023.
12. Chae YK, Chang S, Ko T, Anker J, Agte S, Iams W, Choi WM, Lee K and Cruz M: Epithelial-mesenchymal transition (EMT) signature is inversely associated with T-cell infiltration in non-small cell lung cancer (NSCLC). Sci Rep 8: 2918, 2018.
13. Singh S and Chakrabarti R: Consequences of EMT-driven changes in the immune microenvironment of breast cancer and therapeutic response of cancer cells. J Clin Med 8: 642, 2019.
14. Jiang Y and Zhan H: Communication between EMT and PD-L1 signaling: New insights into tumor immune evasion. Cancer Lett 468: 72-81, 2020.
15. Hasan J, Byers R and Jayson GC: Intra-tumoural microvessel density in human solid tumours. Br J Cancer 86: 1566-1577, 2002.

16. Ning H, Shao QQ, Ding KJ, Gao DX, Lu QL, Cao QW, Niu ZH, Fu Q, Zhang CH, Qu X and Lü JJ: Tumor-infiltrating regulatory T cells are positively correlated with angiogenic status in renal cell carcinoma. Chin Med J (Engl) 125: 2120-2125, 2012.
17. Zhang P, Ma Y, Lv C, Huang M, Li M, Dong B, Liu X, An G, Zhang W, Zhang J, *et al*: Upregulation of programmed cell death ligand 1 promotes resistance response in non-small-cell lung cancer patients treated with neo-adjuvant chemotherapy. Cancer Sci 107: 1563-1571, 2016.
18. Ramser M, Eichelberger S, Däster S, Weixler B, Kraljević M, Mechera R, Tampakis A, Delko T, Güth U, Stadlmann S, *et al*: High OX40 expression in recurrent ovarian carcinoma is indicative for response to repeated chemotherapy. BMC Cancer 18: 425, 2018.
19. Liu X, Huang Y, Qi Y, Wu S, Hu F, Wang J, Shu K, Zhang H, Bartsch JW, Nimsky C, *et al*: The GBM tumor microenvironment as a modulator of therapy response: ADAM8 causes tumor infiltration of tams through HB-EGF/EGFR-mediated CCL2 expression and overcomes TMZ chemosensitization in glioblastoma. Cancers (Basel) 14: 4910, 2022.
20. Malka D, Lièvre A, André T, Taïeb J, Ducreux M and Bibeau F: Immune scores in colorectal cancer: Where are we? Eur J Cancer 140: 105-118, 2020.
21. Kuwahara T, Hazama S, Suzuki N, Yoshida S, Tomochika S, Nakagami Y, Matsui H, Shindo Y, Kanekiyo S, Tokumitsu Y, *et al*: Intratumoural-infiltrating CD4 + and FOXP3 + T cells as strong positive predictive markers for the prognosis of resectable of resectable colorectal cancer. Br J Cancer 121: 659-665, 2019.
22. Bergsland CH, Jeanmougin M, Moosavi SH, Svindland A, Bruun J, Nesbakken A, Sveen A and Lothe RA: Spatial analysis and CD25-expression identify regulatory T cells as predictors of a poor prognosis in colorectal cancer. Mod Pathol 35: 1236-1246, 2022.
23. Sconocchia G, Eppenberger S, Spagnoli GC, Tornillo L, Droeser R, Caratelli S, Ferrelli F, Coppola A, Arriga R, Lauro D, *et al*: NK cells and T cells cooperate during the clinical course of colorectal cancer. Oncoimmunology 3: e952197, 2014.
24. Medrek C, Pontén F, Jirström K and Leandersson K: The presence of tumor associated macrophages in tumor stroma as a prognostic marker for breast cancer patients. BMC Cancer 12: 306, 2012.
25. Pagès F, Mlecnik B, Marliot F, Bindea G, Ou FS, Bifulco C, Lugli A, Zlobec I, Rau TT, Berger MD, *et al*: International validation of the consensus Immunoscore for the classification of colon cancer: A prognostic and accuracy study. Lancet 391: 2128-2139, 2018.
26. Mezheyeuski A, Backman M, Mattsson J, Martín-Bernabé A, Larsson C, Hrynchyk I, Hammarström K, Ström S, Ekström J, Mauchanski S, *et al*: An immune score reflecting pro- and anti-tumoural balance of tumour microenvironment has major prognostic impact and predicts immunotherapy response in solid cancers. EBioMedicine 88: 104452, 2023.
27. Minami K, Hiwatashi K, Ueno S, Sakoda M, Iino S, Okumura H, Hashiguchi M, Kawasaki Y, Kurahara H, Mataki Y, *et al*: Prognostic significance of CD68, CD163 and folate receptor-β positive macrophages in hepatocellular carcinoma. Exp Ther Med 15: 4465-4476, 2018.
28. Yamaguchi T, Fushida S, Yamamoto Y, Tsukada T, Kinoshita J, Oyama K, Miyashita T, Tajima H, Ninomiya I, Munesue S, *et al*: Tumor-associated macrophages of the M2 phenotype contribute to progression in gastric cancer with peritoneal dissemination. Gastric Cancer 19: 1052-1065, 2016.
29. Troiano G, Caponio VCA, Adipietro I, Tepedino M, Santoro R, Laino L, Lo Russo L, Cirillo N and Lo Muzio L: Prognostic significance of $CD68^+$ and $CD163^+$ tumor associated macrophages in head and neck squamous cell carcinoma: A systematic review and meta-analysis. Oral Oncol 93: 66-75, 2019.
30. Shabo I, Olsson H, Sun XF and Svanvik J: Expression of the macrophage antigen CD163 in rectal cancer cells is associated with early local recurrence and reduced survival time. Int J Cancer 125: 1826-1831, 2009.
31. Shabo I, Stål O, Olsson H, Doré S and Svanvik J: Breast cancer expression of CD163, a macrophage scavenger receptor, is related to early distant recurrence and reduced patient survival. Int J Cancer 123: 780-786, 2008.
32. Ma S, Zhao Y, Liu X, Sun Zhang A, Zhang H, Hu G and Sun XF: FCD163 as a potential biomarker in colorectal cancer for tumor microenvironment and cancer prognosis: A Swedish study from tissue microarrays to big data analyses. Cancers (Basel) 14: 6166, 2022.
33. Gorelik L and Flavell RA: Transforming growth factor-beta in T-cell biology. Nat Rev Immunol 2: 46-53, 2002.
34. Thomas DA and Massagué J: TGF-beta directly targets cytotoxic T cell functions during tumor evasion of immune surveillance. Cancer Cell 8: 369-380, 2005.
35. Hao Y, Baker D and Ten Dijke P: TGF-β-mediated epithelial-mesenchymal transition and cancer metastasis. Int J Mol Sci 20: 2767, 2019.
36. Xu J, Lamouille S and Derynck R: TGF-beta-induced epithelial to mesenchymal transition. Cell Res 19: 156-172, 2009.
37. Moustakas A and Heldin CH: Signaling networks guiding epithelial-mesenchymal transitions during embryogenesis and cancer progression. Cancer Sci 98: 1512-1520, 2007.
38. Huang Y, Kim BYS, Chan CK, Hahn SM, Weissman IL and Jiang W: Improving immune-vascular crosstalk for cancer immunotherapy. Nat Rev Immunol 18: 195-203, 2018.
39. Franz L, Alessandrini L, Calvanese L, Crosetta G, Frigo AC and Marioni G: Angiogenesis, programmed death ligand 1 (PD-L1) and immune microenvironment association in laryngeal carcinoma. Pathology 53: 844-851, 2021.
40. Bai Z, Zhou Y, Ye Z, Xiong J, Lan H and Wang F: Tumor-infiltrating lymphocytes in colorectal cancer: The fundamental indication and application on immunotherapy. Front Immunol 12: 808964, 2022.
41. Bruni D, Angell HK and Galon J: The immune contexture and Immunoscore in cancer prognosis and therapeutic efficacy. Nat Rev Cancer 20: 662-680, 2020.
42. Havel JJ, Chowell D and Chan TA: The evolving landscape of biomarkers for checkpoint inhibitor immunotherapy. Nat Rev Cancer 19: 133-150, 2019.
43. Tumeh PC, Harview CL, Yearley JH, Shintaku IP, Taylor EJ, Robert L, Chmielowski B, Spasic M, Henry G, Ciobanu V, *et al*: PD-1 blockade induces responses by inhibiting adaptive immune resistance. Nature 515: 568-571, 2014.
44. Miyamoto Y, Ogawa K, Ohuchi M, Tokunaga R and Baba H: Emerging evidence of immunotherapy for colorectal cancer. Ann Gastroenterol Surg 7: 216-224, 2022.
45. Flecchia C, Zaanan A, Lahlou W, Basile D, Broudin C, Gallois C, Pilla L, Karoui M, Manceau G and Taieb J: MSI colorectal cancer, all you need to know. Clin Res Hepatol Gastroenterol 46: 101983, 2022.